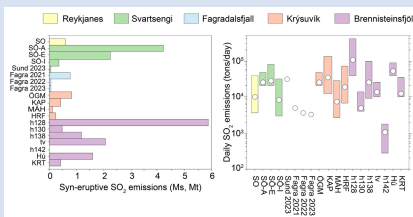# Medieval and recent SO$_2$ budgets in the Reykjanes Peninsula: implication for future hazard

A. Caracciolo[1*], E. Bali[1], E. Ranta[2], S.A. Halldórsson[1], G.H. Guðfinnsson[1], B.V. Óskarsson[3]

OPEN ACCESS

Abstract

Exposure to volcanic SO$_2$ can have adverse effects on human health, with severe respiratory disorders documented on short- and long-term timescales. Here, we use melt inclusion and groundmass glass data to calculate potential syneruptive SO$_2$ emissions during medieval and recent (2021–2024) eruptions across the Reykjanes Peninsula, the most populated area of Iceland, which has recently undergone magmatic reactivation with the 2021–2024 eruptions at Fagradalsfjall and Svartsengi. We target 16 individual eruptions from the medieval volcanic cycle at the Reykjanes Peninsula, the 800–1240 AD Fires, along with the 2021–2023 Fagradalsfjall eruptions and the 2023–2024 eruptions at Sundhnúksgígar. We calculate potential SO$_2$ emissions across the RP for the individual eruptions to be in the range of 0.004–6.3 Mt. These estimates correspond to mean daily SO$_2$ emissions in the range of 1000–111,000 t/day, higher than the mean SO$_2$ measurements of 5240 ± 2700 t/day during the 2021 Fagradalsfjall eruption. By using pre-eruptive sulfur values preserved in undegassed melt inclusions, we develop an empirical approach to calculate best- and worst-case potential SO$_2$ emission scenarios of any past or ongoing Reykjanes Peninsula eruption of known effusion rate. We conclude that the potential sulfur emissions across the RP can be significantly higher than observed during the 2021 Fagradalsfjall eruption, mainly because of the more evolved nature and higher sulfur contents of magmas erupted during the medieval period. Based on dominant NW wind directions on the Reykjanes Peninsula, eruptions in Brennisteinsfjöll pose the greatest health hazard to the capital area. Sulfate aerosol produced during long-term eruptions may impact visibility and air quality in the Keflavík Airport area. Our findings enable assessment of SO$_2$ emission scenarios of future eruptions across the RP and can be used together with gas dispersal models to forecast SO$_2$ pollution at ground level, and its impact on human health.

Introduction

The release of volcanic gases and aerosols during volcanic eruptions can significantly impact the air quality and climate (*e.g.*, Ilyinskaya *et al.*, 2017), as well as biodiversity (*e.g.*, Weiser *et al.*, 2022). Among volcanic gases, sulfur species (SO$_2$, H$_2$S) and associated aerosols (SO$_4$, H$_2$SO$_4$) are the most critical airborne hazards to human health, with short- and long-term impacts that have been recorded at variable distances from eruptive vents (*e.g.*, Schmidt *et al.*, 2015; Ilyinskaya *et al.*, 2017; Stewart *et al.*, 2022; Horwell *et al.*, 2023). For example, several studies have associated cardiorespiratory issues with volcanic sulfur emissions (*e.g.*, Carlsen *et al.*, 2021, and references therein). Hence, a detailed knowledge of potential sulfur releases of active volcanoes located in densely populated areas is critical to understand air quality hazards of future volcanic eruptions. This is the case of the Reykjanes Peninsula (RP) in southwest Iceland, an active spreading area segmented into five volcanic systems, which from west to east are Reykjanes, Svartsengi, Fagradalsfjall, Krýsvík and Brennisteinsfjöll. The latest magmatic period in the RP occurred ~800 years ago (Sæmundsson *et al.*, 2020), but knowledge about sulfur outputs during those

eruptions has been lacking thus far. Each volcanic system on the RP tends to activate during individual magmatic periods (Sæmundsson *et al.*, 2020), and the recent 2021–2024 Fagradalsfjall and Svartsengi eruptions (Barsotti *et al.*, 2023; Sigmundsson *et al.*, 2024) suggest the potential initiation of a new eruptive period in an area that hosts ~70 % of the Icelandic population. Consequently, there is an increased societal need for a deeper understanding of sulfur emissions across the RP, which is crucial for a comprehensive assessment of sulfur's impact during future eruptions and its potential consequences for human health.

Here, we focus on magmatic units erupted in the volcanic systems of Reykjanes, Svartsengi, Krýsvík and Brennisteinsfjöll in the RP during the last medieval eruptive cycle, which occurred between the 8th century and 1240 AD, hereafter referred to as the 800–1240 AD Fires (Peate *et al.*, 2009; Caracciolo *et al.*, 2023). Additionally, we target the 2021–2023 Fagradalsfjall eruptions and the December 2023, January 2024 and February 2024 eruptions at Sundhnúksgígar in Svartsengi. We calculate syn-eruptive sulfur release and potential sulfur emissions of 19 geologically and petrochemically well characterised magmatic

1. NordVulk, Institute of Earth Sciences, University of Iceland, 102, Reykjavík, Iceland
2. Department of Geosciences and Geography, University of Helsinki, 00014, Helsinki, Finland
3. Icelandic Institute of Natural History, 210, Garðabær, Iceland

* Corresponding author (email: alberto@hi.is)

units (Peate *et al.*, 2009; Caracciolo *et al.*, 2023) and compare those with sulfur emissions from the 2021 Fagradalsfjall eruption (Halldórsson *et al.*, 2022; Barsotti *et al.*, 2023). Also, we estimate daily SO$_2$ emissions and develop an empirical approach to calculate worst- and best-case potential sulfur emissions for any eruption of a given volume emplaced in the RP.

Samples and Methods

Scoria samples were collected from multiple vents within individual eruptive units of the 800–1240 AD Fires (Table S-1) (Caracciolo *et al.*, 2023). Here, we present new sulfur (S) data for the same groundmass glass ($n = 889$) and melt inclusions (MIs) ($n = 416$) dataset published in Caracciolo *et al.* (2023). Additionally, we include new MI and groundmass glass data from quenched lavas and tephra erupted during the 2022 and 2023 Fagradalsfjall eruptions, as well as data from the eruptions at Sundhnúksgígar that occurred in the Svartsengi volcanic system in December 2023, January 2024 and February 2024. S was analysed by electron microprobe analyser (EMPA) at the University of Iceland, using the same analytical settings as in Caracciolo *et al.* (2020), and MI compositions have been corrected for post-entrapment processes (PEP) (Tables S-2–S-4) (Caracciolo *et al.*, 2023).

Here, we use the 'petrological method' (Devine *et al.*, 1984) to calculate eruptive sulfur emissions based on the difference between S concentrations in mineral-hosted MIs and S concentrations measured in groundmass glass (ΔC_S). The idea behind this reconstruction method is that melt inclusions with similar composition to erupted melts preserve the pre-eruptive volatile content, and quenched groundmass glasses provide an estimate of the post-eruptive volatile content. For the different magmatic units, the highest S concentration measured in PEP-corrected MIs ($C_{S\ MI}$) is selected as the pre-eruptive S concentration, whereas the lowest S concentration in groundmass glasses ($C_{S\ glass}$) is chosen as the post-eruptive S concentration. By combining the mass of erupted magmas with the mass of S released, we can assess vent syneruptive SO$_2$ emissions (M_S) of individual eruptions (see Eqs. S-1, S-2) (*e.g.*, Bali *et al.*, 2018, and references therein). Furthermore, we calculate the magnitude of potential SO$_2$ emissions (potential M_S), which refers to complete degassing of all pre-eruptive sulfur ($C_{S\ glass} = 0$) and reflects the maximum amount of SO$_2$ that a specific eruption could potentially have released, assuming that there is no degassing of unerupted magma. This reconstruction method has been shown to have matched field-based volatile measurements exceptionally well during the 2014–2015 Holuhraun eruption (Bali *et al.*, 2018; Pfeffer *et al.*, 2018) and the 2021 Fagradalsfjall eruption (this work, Table 1).

Sulfur Concentrations in MIs and Groundmass Glass

Sulfur concentration in MIs is in the range of 200–1900 ppm, with a relatively large variability of S at a given MI Mg#. Particularly, the most primitive MIs (Mg# > 65), exclusively preserved in Reykjanes and Krýsuvík, record S contents in the range of 580–1070 ppm (Fig. 1). S concentration in PEP-corrected MI compositions increases with decreasing MI Mg#, as expected for melt compositions controlled by fractional crystallisation. MIs from the 2023–2024 eruptions at Sundhnúksgígar record pre-eruptive S concentrations in the range of 1400–1600 ppm, in agreement with MI data from the medieval eruptions (Fig. 1b). MIs from the 2022–2023 Fagradalsfjall eruptions closely match S concentrations

measured in the 2021 products (Fig. 1c). Groundmass glasses from Brennisteinsfjöll have mean S contents in the range of 150–280 ppm, lower than mean S contents measured in glasses from the other volcanic systems (280–450 ppm) (Fig. 1, Table 1). For comparison, MIs from the 2021 Fagradalsfjall eruption contain maximum S concentrations of 1200 ppm, whereas the groundmass glasses contain 20–200 ppm S. Sulfide globules were not observed in the erupted samples.

Assessing Sulfur Variability and Degassing during the 800–1240 AD Fires

Considering that medieval and recent eruptions on the RP are likely sourced from mantle-derived melts of diverse compositions (Peate *et al.*, 2009; Halldórsson *et al.*, 2022; Harðardóttir *et al.*, 2022; Caracciolo *et al.*, 2023), including melts with variable S contents (Ranta *et al.*, 2022), we use our MI record to estimate S contents of the local enriched and depleted end member melt components. We distinguish between these components from the K$_2$O/TiO$_2$ variability, a robust tracer of mantle heterogeneities in Iceland (Halldórsson *et al.*, 2022; Harðardóttir *et al.*, 2022) (see Supplementary Information). Our modelling, considering that S behaves as an incompatible element in basaltic magmas, shows that most of the MI S variability can be explained by fractional crystallisation (FC) and mixing of, at least, two end member melt compositions (Fig. 1a–d).

In order to evaluate S saturation during magma ascent and fractional crystallisation through the crust, we calculate sulfur content at sulfide saturation (SCSS) along a FC path, which reflects the amount of S^{2-} present in a melt in equilibrium with a sulfide phase (Smythe *et al.*, 2017) (see Supplementary Information). Our modelling suggests that melts are sulfide undersaturated during most of magmatic fractionation across the RP (Figs. 1, S-3, S-4). Only magmas from Svartsengi and Brennisteinsfjöll have a high likelihood to be sulfide saturated prior to eruptions. Furthermore, sulfide saturation is reached earlier during magmatic differentiation of enriched mantle-derived melts than depleted melts (Fig. 1).

Modelling of S degassing with Sulfur_X (Ding *et al.*, 2023) suggests that the basaltic melts that erupted during the 800–1240 AD Reykjanes Fires are unlikely to degas significant amounts of S at known pre-eruptive magma storage depths (Caracciolo *et al.*, 2023) and that significant S degassing only takes place during magma ascent in the last 0.2 kbar (<700 m) (Fig. S-1).

Sulfur Emissions across the RP

Sulfur release ranges between 1000 and 1770 ppm across the RP, a typical range for Icelandic rift basalts (Ranta *et al.*, 2024), with the largest ΔC_S found in lavas from Svartsengi and Brennisteinsfjöll (Table 1). ΔC_S values can be scaled by the mass of erupted material to estimate M_S of individual eruptions, using published volumes of individual eruptive units, in the range of 0.01 km^3 to 0.72 km^3 (Table 1). Using a melt density of 2700 kg/m^3 and assuming a bulk vesicularity of 15 vol. %, we calculate M_S between 0.003 and 5.9 Mt (Fig. 2a). The most voluminous lavas found in Svartsengi and Brennisteinsfjöll released the highest mass of SO$_2$ into the atmosphere during the medieval period. The syneruptive SO$_2$ released by these latter voluminous lavas is approximately 2 to 6 times larger than syneruptive SO$_2$ emissions during the 2021 Fagradalsfjall eruption, for which we estimated $M_S = 0.78$ Mt ($M_{S\ measured} = 0.97 \pm 0.5$; Barsotti *et al.*, 2023). These are roughly between 20 and 70 % of the syneruptive SO$_2$ emissions estimated for the 2014–2015 Holuhraun eruption ($M_S = 10.5$ Mt; Bali *et al.*, 2018). We calculate SO$_2$ release of

Table 1 Eruptive units studied in this work and summary of main results. $C_{S\,MI}$, pre-eruptive S concentration; $C_{S\,glass}$, post-eruptive S concentration; ΔC_S, sulfur emissions at the vent *per* unit mass of melt, accounting for crystallinity; V, bulk lava volume; V_{DRE}, vesicle-free lava volume; M_S, syneruptive SO_2 emissions at the vent; potential M_S, potential SO_2 emissions at the vent; MOR, mean output rates. Lava volumes for the medieval eruptions are from Einarsson *et al.* (1991), Jónsson (1978) and Sigurgeirsson (2004). 'No.' indicates the number of eruptive units, as indicated in Figure 3.

No.	Eruptive unit	Acronym	Volcanic system	Age A.D.	$C_{S\,MI}$ ppm	$C_{S\,glass}$ ppm	ΔC_S ppm	V km³	V_{DRE} km³	Mass Kg	M_S Mt	Potential M_S Mt	MOR[b] m³/s	Time of lava emplacement days	Daily SO_2 emissions t/day
1	Stampahraun 4	SO	Reykjanes	1210–1240	1559	258	1275	0.10	0.09	2.3E+11	0.58	0.71	6.4–67.9 (17.9)	17–193 (65)	3570–40,450 (10,620)
2	Arnarseturshraun	SÖ-A	Svartsengi	1210–1240	1907	196	1667	0.55	0.47	1.3E+12	4.23	4.81	26.1–60.1 (33.5)	106–244 (190)	20,420–47,000 (26,200)
3	Eldvarpahraun	SÖ-E	Svartsengi	1210–1240	1907	112	1759	0.28	0.24	6.4E+11	2.26	2.45	26–93.7 (33.3)	35–125 (97)	21,340–76,900 (27,300)
4	Illahraun	SÖ-I	Svartsengi	1210–1240	1907	312	1563	0.05	0.04	1.1E+11	0.36	0.44	4–42.7 (11.2)	14–145 (52)	2920–31,140 (8180)
5	Sundhnúkar Dec. 2023	Sund 2023	Svartsengi	2023	1610	210	1372	0.011[d]	0.01	2.5E+10	0.07	0.08	50[d]	2.5	32,000
6	Sundhnúkar Jan. 2024*	Sund 2024a	Svartsengi	2024	1400	160	1215	-	-	-	-	-	-	<2	-
7	Sundhnúkar Feb. 2024*	Sund 2024b	Svartsengi	2024	1607	164	1414	-	-	-	-	-	-	<2	-
8	Fagradalsfjall 2021	Fagra 2021	Fagradalsfjall	2021	1170	20	1127	0.15[c]	0.13	4.1E+11	0.78	0.80	9.5[c]	185	5000
9	Fagradalsfjall 2022	Fagra 2022	Fagradalsfjall	2022	1300	120	1180	0.011[d]	0.01	2.5E+10	0.06	0.07	7.0[d]	18	3780
10	Fagradalsfjall 2023	Fagra 2023	Fagradalsfjall	2023	1170	120	1050	0.015[d]	0.013	3.4E+10	0.07	0.08	7.0[d]	26	3360
11	Ögmundarhraun	ÖGM	Krýsuvík	1151–1188	1517	138	1351	0.13	0.11	3.0E+11	0.81	0.90	31.9–73.3 (40.8)	21–47 (37)	20,110–46,220 (25,750)
12	Kapelluhraun	KAP	Krýsuvík	1151–1188	1482	183	1273	0.07	0.06	1.6E+11	0.41	0.48	20.2–213 (56)	4–40 (14)	12,000–126,500 (33,240)
13	Mávahlíðarhraun	MÁH	Krýsuvík	1151–1188	1297	280	997	0.02	0.02	4.6E+10	0.09	0.12	5.8–61 (16)	4–40 (14)	2700–28,370 (7450)
14	Hrútafellshraun[a]	HRF	Krýsuvík	8th–9th century	1546	252	1268	0.04[a]	0.03	9.0E+10	0.23	0.28	11.4–120 (31.5)	4–40 (14)	6750–71,000 (18,660)
15	Hvammahraun	h128	Brennisteinsfjöll	8th–9th century	1900	90	1810	0.72	0.61	1.7E+12	5.86	6.27	48.3–510.6 (134.1)	16–173 (62)	39,970–422,560 (111,000)
16	Kistuhraun	h130	Brennisteinsfjöll	900–1100	1494	94	1372	0.08	0.07	1.8E+11	0.50	0.55	6.1–22 (7.8)	42–152 (119)	3900–14,000 (5000)
17	Selvogshraun	h138	Brennisteinsfjöll	10th–11th century	1504	126	1350	0.19	0.16	4.4E+11	1.18	1.31	14.2–149.9 (39.4)	15–155 (56)	8950–94,450 (24,810)
18	Tvíbollahraun	tv	Brennisteinsfjöll	950	1367	129	1213	0.37	0.31	8.5E+11	2.06	2.32	18.7–43 (24)	100–229 (178)	10,580–24,340 (13,580)
19	Svartihryggur[a]	h142	Brennisteinsfjöll	900–1200	1341	147	1170	0.0005[a]	0.0004	1.3E+09	0.003	0.003	0.5–3.3 (2)	2–13 (3)	270–1800 (1100)
20	Húsfellsbruni[a]	Hú1 & Hú2	Brennisteinsfjöll	9th–13th century	1739	55	1650	0.20[a]	0.17	4.9E+11	1.62	1.70	50.6–116.4 (64.9)	21–49 (38)	38,960–89,620 (50,000)
21	Kristnitökuhraun[a]	KRT	Brennisteinsfjöll	1000	1640	118	1492	0.06[a]	0.05	1.4E+11	0.41	0.45	14.1–50.9 (18)	14–50 (39)	9800–35,420 (12,570)

[a] Lava volume estimated by assuming a thickness of 5 m, consistent with average thicknesses of lava flows of known volumes with a similar aerial extent.

[b] MOR values (within brackets) and uncertainty ranges for the medieval eruptions are from Óskarsson *et al.* (2024).

[c] V and MOR from Pedersen *et al.* (2022).

[d] V and MOR from Pedersen *et al.* (2024).

* Lava volumes for the 2024 eruptions at Sundhnúksgígar are not available at the current stage.
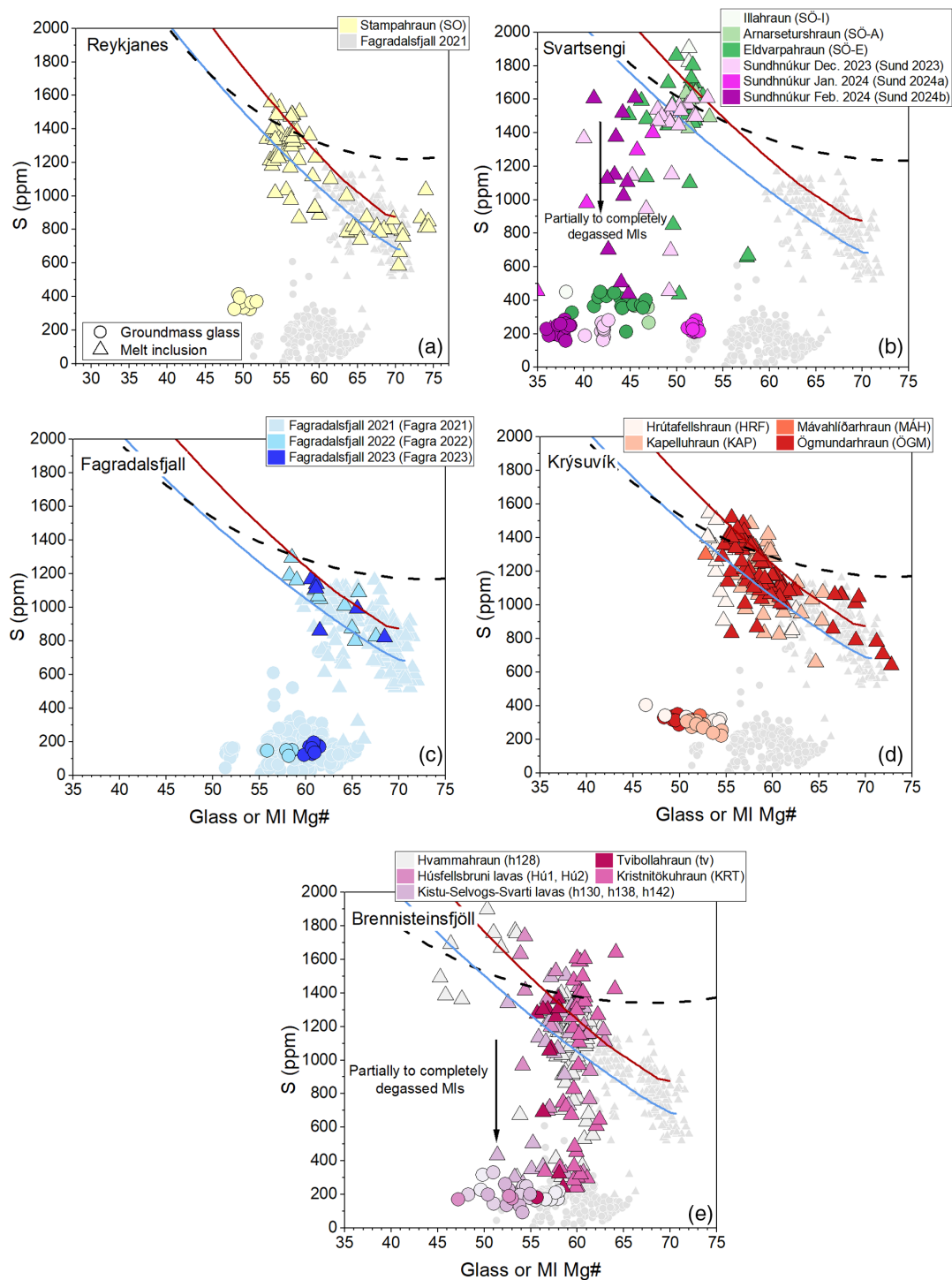
Figure 1 Variations of S contents in groundmass glasses (filled circles) and PEP-corrected MIs (filled triangles) as a function of Mg# [Mg# = $100 \cdot Mg/(Mg+Fe^{2+})$, $Fe^{2+}/Fe^{tot} = 0.9$] in samples from **(a,b,d,e)** the 800–1240 AD Fires, **(c)** the 2021–2023 Fagradalsfjall eruptions and **(b)** the 2023–2024 eruptions at Sundhnúksgígar. Data from the 2021 Fagradalsfjall eruption are from Halldórsson *et al.* (2022). Red and blue solid lines indicate fractional crystallisation paths calculated for geochemically enriched and depleted initial melt compositions, respectively (see Supplementary Information). The black dotted curve indicates SCSS along an empirical fractional crystallisation path calculated after Smythe *et al.* (2017), implemented in PySulfSat (Wieser and Gleeson, 2022).

0.06–0.07 Mt for the 2022 and 2023 Fagradalsfjall eruptions, respectively. However, for a given mass of melt, the 2021–2023 Fagradalsfjall eruptions released a comparable mass of SO_2 (Table 1). Conversely, the 2023–2024 eruptions at Sundhnúksgígar slightly exceeded SO_2 emissions during the 2021–2023 Fagradalsfjall eruptions (Table 1). Similarly, we have calculated

potential M_S, the maximum mass of SO_2 that could potentially have been released during each eruption. Potential M_S across the RP ranges between 0.003 and 6.3 Mt and is only slightly higher than vent M_S, as most of the S is released into the atmosphere during eruptions rather than staying dissolved in the lava (Table 1).
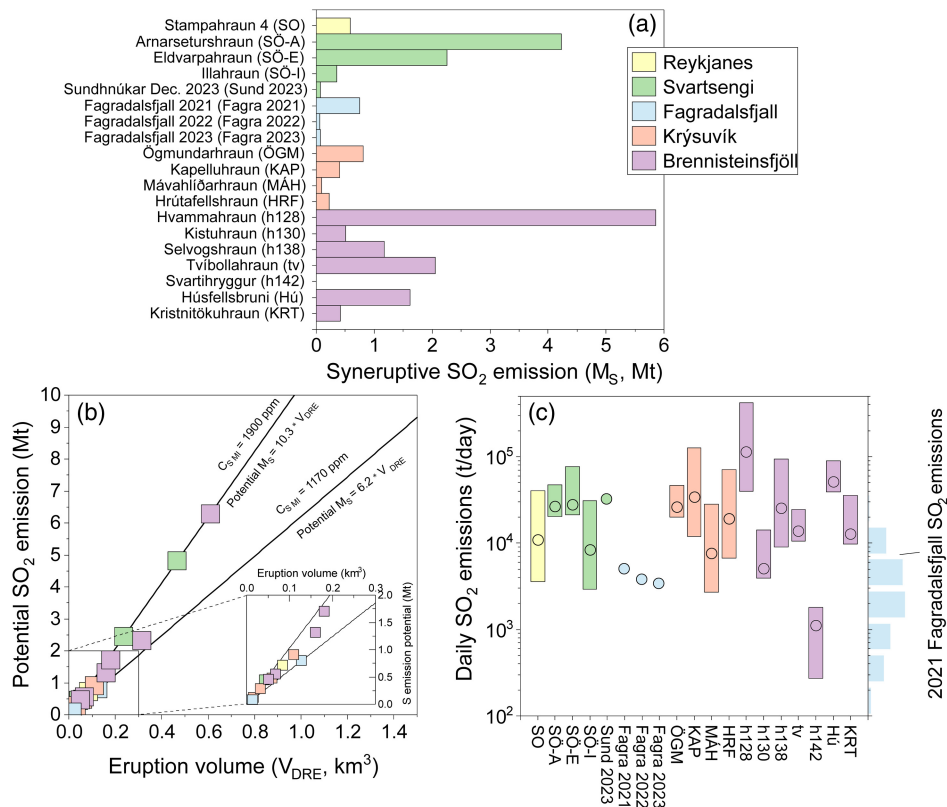
Figure 2 **(a)** Variation of vent M_S. **(b)** Magnitude of potential M_S as a function of eruption volume for the 800–1240 AD Fires, the 2021–2023 Fagradalsfjall eruptions and the 2023 Sundhnúkar eruption. At a given volume, straight lines allow to calculate potential M_S corresponding to maximum and minimum pre-eruptive S concentrations measured across the RP. Inset plot shows most common potential M_S across the RP. **(c)** Daily SO_2 emissions are calculated using MOR values and associated uncertainties from Óskarsson et al. (2024). Blue histogram indicates measured SO_2 emissions during the 2021 Fagradalsfjall eruption (Esse et al., 2023). Data are coloured according to the volcanic system and only lavas with known volumes or MORs are included in the plots.

Evaluating End Member Scenarios of SO_2 Emissions and Hazard Potential for Future Eruptions across the RP

Based on the MI record of the 2021–2023 Fagradalsfjall eruptions (Halldórsson et al., 2022; this work), the 2023–2024 eruptions at Sundhnúksgígar and the 800–1240 AD Fires (this work), we constrain potential maximum (1900 ppm) and minimum (1170 ppm) pre-eruptive S concentrations and use these to estimate potential M_S of future eruptions in the RP. With these constraints, we developed an empirical approach to assess potential M_S for a given eruption of known lava volume, with important applications for forecasting the worst- and best-case scenarios of potential M_S of future eruptive events (Fig. 2b). For example, based on our approach, an eruption with an eruptive volume of 0.4 km³ could release between 2.9 Mt and 4.1 Mt SO_2. This method also has an application when it comes to evaluating the long-term SO_2 impact of ongoing eruptions in the RP. If the mean magma output rate (MOR) is known and fixed, one can roughly estimate the volume of the lava flow and calculate potential M_S at any given moment from the onset of the eruption. This provides a valuable tool to assess best- and worst-case scenarios for SO_2 pollution during ongoing events.

Eruptive M_S calculations are strongly dependent on lava flow volumes. Hence, when it comes to comparing the 800–1240 AD Fires with the 2021–2024 eruptions, a more relevant parameter is the mean daily SO_2 emissions, which also is an important parameter from a hazard perspective. We have estimated daily SO_2 emissions for the 800–1240 AD Fires using MOR values calculated by Oskarsson et al. (2024), in the range

of 3–119 m³/s (Table 1, Eq. S-3). Mean daily SO_2 emissions during the medieval eruptions likely ranged between 1000 t/day and 111,000 t/day (Fig. 2c). In comparison, during the 2021, 2022 and 2023 Fagradalsfjall eruptions, we calculate average daily SO_2 emissions of 5000, 3780 and 3360 t/day, respectively. The estimate for the 2021 Fagradalsfjall eruption is in agreement with the majority of measured daily SO_2 emissions throughout the 2021 Fagradalsfjall eruption, in the range of 1000–7600 t/day (Esse et al., 2023), and with daily SO_2 emissions of 5240 ± 2700 t/day, calculated assuming 0.97 ± 0.5 Mt total mass of SO_2 (Barsotti et al., 2023). In contrast, the December 2023 Sundhnúkar eruption released 32,000 t/day SO_2 (Table 1). Our calculations highlight that future eruptions in the RP may have the potential to release significantly more SO_2 on a daily basis than the 2021–2024 eruptions.

SO_2 emissions during the 800–1240 AD Fires and the 2021–2024 eruptions are small compared to those during the 2014–2015 Holuhraun basaltic eruption (9.2 Mt SO_2; Pfeffer et al., 2018). However, volcanic eruptions in the RP are potentially considered to be more hazardous due to their proximity to inhabited areas, to the international airport and to the large number of visitors expected at eruption sites (Fig. 3) (Barsotti et al., 2023). To assess the health hazard for potential future eruptions, we built seasonal wind roses, for the period 2012–2022, reflecting dominant wind speeds and directions in the RP (Hersbach et al., 2023). We find that, most of the time, prevailing winds blow towards the NW–NE, suggesting different SO_2 health hazard potentials associated with eruptions within different volcanic systems (Fig. 3). The prevalent NW wind blowing direction suggests that volcanic SO_2 emissions could still be disruptive to the Keflavik Airport area if there were a long-duration eruption.
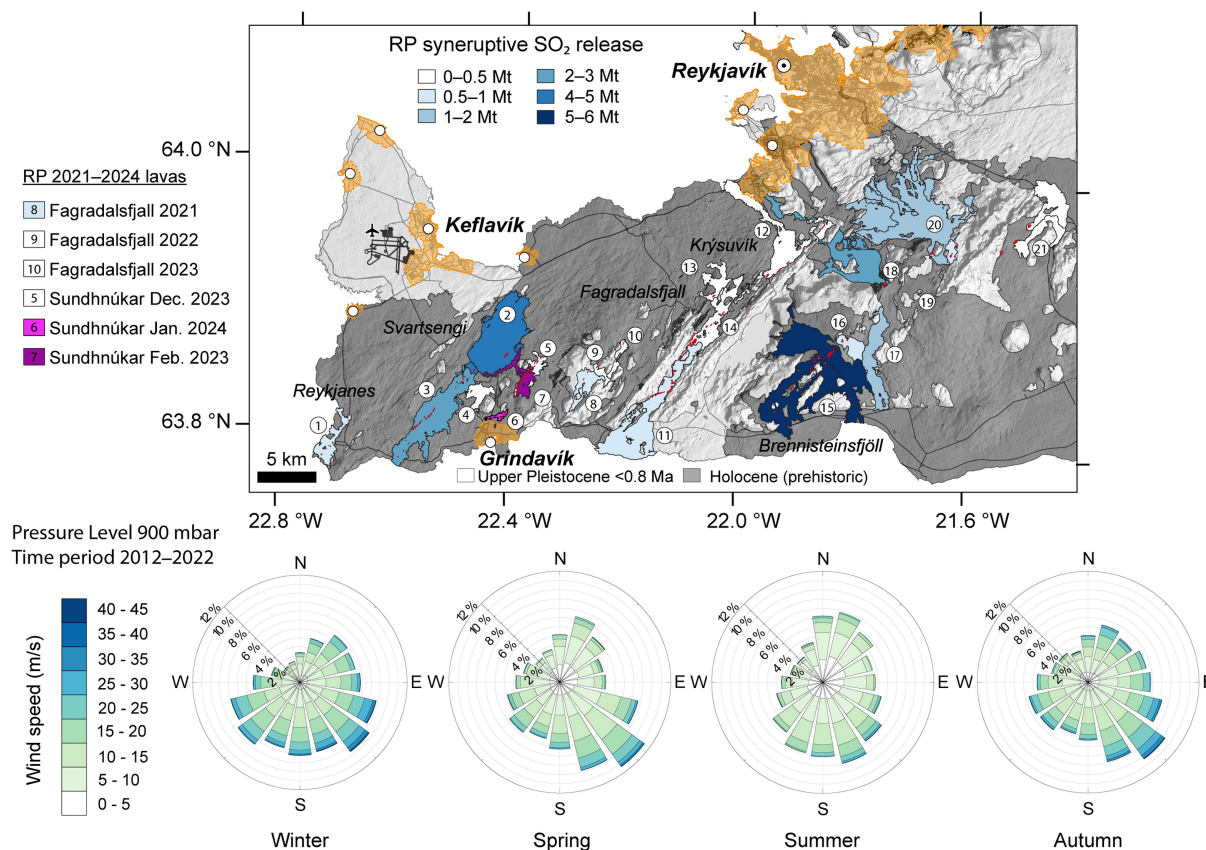
Figure 3 Simplified geological map of the RP and lava flows emplaced during the 800–1240 AD Fires. The map also illustrates the aerial extent of the 2021 (Pedersen *et al.*, 2022), 2022 (Gunnarson *et al.*, 2023) and 2023 (Belart *et al.*, 2023) Fagradalsfjall lavas. Data from the 2023–2024 eruptions at Sundhnúksgígar are from the Landmælingar Íslands geoserver (gis.lmi.is/geoserver). When possible, lava flows are coloured according to calculated syneruptive SO_2 emissions, ranging from 0.1 to 6 Mt. Orange shaded areas indicate urban areas. Numbers reflect the different erupted units as listed in Table 1. Seasonal wind roses reflect data at 900 mPa (~1000 m a.s.l), which was the most common SO_2 injection altitude during the 2021 Fagradalsfjall eruption (Esse *et al.*, 2023). Spokes indicate the direction the wind is blowing from, and the length of each spoke shows the frequency. Wind data were extracted from ERA5 (Hersbach *et al.*, 2023).

Even if eruptions in the RP produce little ash, sulfate aerosol in the atmosphere could reduce visibility and air quality (Pattantyus *et al.*, 2018). Eruptions in Brennisteinsfjöll are the most hazardous for Reykjavík, especially in spring and autumn seasons, as SO_2 is likely to be blown towards the capital area. Eruptions in Reykjanes pose a minimal hazard as winds tend to blow away from inhabited areas. During assessment of possible eruptive scenarios in the RP, our estimates provide key input parameters to model the release and dispersion of volcanic SO_2 into the atmosphere. Our results can be used to inform SO_2 pollution hazard assessments for potential eruptive scenarios and prompt action and mitigation plans during ongoing volcanic crises in the RP.

Acknowledgements

Additional Information

References

Bali, E., Hartley, M.E., Halldórsson, S.A., Gudfinnsson, G.H., Jakobsson, S. (2018) Melt inclusion constraints on volatile systematics and degassing history of the 2014–2015 Holuhraun eruption, Iceland. *Contributions to Mineralogy and Petrology* 173, 9. https://doi.org/10.1007/s00410-017-1434-1

Barsotti, S., Parks, M.M., Pfeffer, M.A., Óladóttir, B.A., Barnie, T., Titos, M.M., Jónsdóttir, K., Pedersen, G.B.M., Hjartardóttir, Á.R., Stefansdóttir, G., Johannsson, T., Arason, P., Gudmundsson, M.T., Oddsson, B.,

Þrastarson, R.H., Ófeigsson, B.G., Vogfjörd, K., Geirsson, H., Hjörvar, T., von Löwis, S., Petersen, G.N., Sigurðsson, E.M. (2023) The eruption in Fagradalsfjall (2021, Iceland): how the operational monitoring and the volcanic hazard assessment contributed to its safe access. *Natural Hazards* 116, 3063–3092. https://doi.org/10.1007/s11069-022-05798-7

Belart, J.M.C., Pinel, V., Reynolds, H.I., Berthier, E., Gunnarson, S.R. (2023) Digital Elevation Models (DEMs) and lava outlines from the 2023 Litla-Hrútur eruption, Iceland, from Pléiades satellite stereoimages [Data set]. *Zenodo*. https://doi.org/10.5281/zenodo.10133203

Caracciolo, A., Bali, E., Guðfinnsson, G.H., Kahl, M., Halldórsson, S.A., Hartley, M.E., Gunnarsson, H. (2020) Temporal evolution of magma and crystal mush storage conditions in the Bárðarbunga-Veiðivötn volcanic system, Iceland. *Lithos* 352–353, 105234. https://doi.org/10.1016/j.lithos.2019.105234

Caracciolo, A., Bali, E., Halldórsson, S.A., Guðfinnsson, G.H., Kahl, M., Þórðardóttir, I., Pálmadóttir, G.L., Silvestri, V. (2023) Magma plumbing architectures and timescales of magmatic processes during historical magmatism on the Reykjanes Peninsula, Iceland. *Earth and Planetary Science Letters* 621, 118378. https://doi.org/10.1016/j.epsl.2023.118378

Carlsen, H.K., Valdimarsdóttir, U., Briem, H., Dominici, F., Finnbjornsdottir, R.G., Jóhannsson, T., Aspelund, T., Gislason, T., Gudnason, T. (2021) Severe volcanic SO₂ exposure and respiratory morbidity in the Icelandic population – a register study. *Environmental Health* 20, 23. https://doi.org/10.1186/s12940-021-00698-y

Devine, J.D., Sigurdsson, H., Davis, A.N., Self, S. (1984) Estimates of sulfur and chlorine yield to the atmosphere from volcanic eruptions and potential climatic effects. *Journal of Geophysical Research: Solid Earth* 89, 6309–6325. https://doi.org/10.1029/JB089iB07p06309

Ding, S., Plank, T., Wallace, P.J., Rasmussen, D.J. (2023) Sulfur_X: A Model of Sulfur Degassing During Magma Ascent. *Geochemistry, Geophysics, Geosystems* 24, e2022GC010552. https://doi.org/10.1029/2022GC010552

Einarsson, S., Johannesson, H., Sveinbjörnsdóttir, Á.E. (1991) Krísuvíkureldar II. Kapelluhraun og gátan um aldur Hellnahrauns. *Jökull* 41, 61–80. https://doi.org/10.33799/jokull1991.41.061

Esse, B., Burton, M., Hayer, C., Pfeffer, M.A., Barsotti, S., Theys, N., Barnie, T., Titos, M. (2023) Satellite derived SO₂ emissions from the relatively low-intensity, effusive 2021 eruption of Fagradalsfjall, Iceland. *Earth and Planetary Science Letters* 619, 118325. https://doi.org/10.1016/j.epsl.2023.118325

Gunnarson, S.R., Belart, J.M.C., Óskarsson, B.V., Gudmundsson, M.T., Högnadóttir, T., Pedersen, G.B.M., Dürig, T., Pinel, V. (2023) Automated processing of aerial imagery for geohazards monitoring: Results from Fagradalsfjall eruption, SW Iceland, August 2022 [Dataset]. *Zenodo*. https://doi.org/10.5281/zenodo.7871187

Halldórsson, S.A., Marshall, E.W., Caracciolo, A., Matthews, S., Bali, E., Rasmussen, M.B., Ranta, E., Robin, J.G., Guðfinnsson, G.H., Sigmarsson, O., Maclennan, J., Jackson, M.G., Whitehouse, M.J., Jeon, H., van der Meer, Q.H.A., Mibei, G.K., Kalliokoski, M.H., Repczynska, M.M., Rúnarsdóttir, R.H., Sigurðsson, G., Pfeffer, M.A., Scott, S.W., Kjartansdóttir, R., Kleine, B.I., Oppenheimer, C., Aiuppa, A., Ilyinskaya, E., Bitetto, M., Giudice, G., Stefánsson, A. (2022) Rapid shifting of a deep magmatic source at Fagradalsfjall volcano, Iceland. *Nature* 609, 529–534. https://doi.org/10.1038/s41586-022-04981-x

Harðardóttir, S., Matthews, S., Halldórsson, S.A., Jackson, M.G. (2022) Spatial distribution and geochemical characterization of Icelandic mantle end-members: Implications for plume geometry and melting processes. *Chemical Geology* 604, 120930. https://doi.org/10.1016/j.chemgeo.2022.120930

Hersbach, H., Bell, B., Berrisford, P., Biavati, G., Horányi, A., Muñoz Sabater, J., Nicolas, J., Peubey, C., Radu, R., Rozum, I., Schepers, D., Simmons, A., Soci, C., Dee, D., Thépaut, J.-N. (2023) ERA5 hourly data on pressure levels from 1940 to present. *Copernicus Climate Change Service (C3S) Climate Data Store (CDS)*. Accessed 26 October 2023. https://doi.org/10.24381/cds.bd0915c6

Horwell, C.J., Baxter, P.J., Damby, D.E., Elias, T., Ilyinskaya, E., Sparks, R.S.J., Stewart, C., Tomašek, I. (2023) The International Volcanic Health Hazard Network (IVHHN): reflections on 20 years of progress. *Frontiers in Earth Science* 11, 1213363. https://doi.org/10.3389/feart.2023.1213363

Ilyinskaya, E., Schmidt, A., Mather, T.A., Pope, F.D., Witham, C., Baxter, P., Jóhannsson, T., Pfeffer, M., Barsotti, S., Singh, A., Sanderson, P., Bergsson, B., McCormick Kilbride, B., Donovan, A., Peters, N., Oppenheimer, C., Edmonds, M. (2017) Understanding the environmental impacts of large fissure eruptions: Aerosol and gas emissions from the 2014–2015 Holuhraun eruption (Iceland). *Earth and Planetary Science Letters* 472, 309–322. https://doi.org/10.1016/j.epsl.2017.05.025

Jónsson, J. (1978) *Jarðfræðikort af Reykjanesskaga : 1. Skýringar við jarðfræðikort ; 2. Jarðfræðikort*. Orkustofnun jarðhitadeild, Reykjavík. http://hdl.handle.net/10802/4981

Óskarsson, B.V., Askew, R.A., Guðmundsson, H. (2024) Assessing the mean output rate (MOR) of past effusive basaltic eruptions - a look at the postglacial volcanism of the Reykjanes Peninsula in Iceland. *EarthArXiv* Preprint v1. https://doi.org/10.31223/X5CH68

Pattantyus, A.K., Businger, S., Howell, S.G. (2018) Review of sulfur dioxide to sulfate aerosol chemistry at Kīlauea Volcano, Hawai'i. *Atmospheric Environment* 185, 262–271. https://doi.org/10.1016/j.atmosenv.2018.04.055

Peate, D.W., Baker, J.A., Jakobsson, S.P., Waight, T.E., Kent, A.J.R., Grassineau, N.V., Skovgaard, A.C. (2009) Historic magmatism on the Reykjanes Peninsula, Iceland: a snap-shot of melt generation at a ridge segment. *Contributions to Mineralogy and Petrology* 157, 359–382. https://doi.org/10.1007/s00410-008-0339-4

Pedersen, G.B.M., Belart, J.M.C., Óskarsson, B.V., Gudmundsson, M.T., Gies, N., Högnadóttir, T., Hjartardóttir, Á.R., Pinel, V., Berthier, E., Dürig, T., Reynolds, H.I., Hamilton, C.W., Valsson, G., Einarsson, P., Ben-Yehosua, D., Gunnarsson, A., Oddsson, B. (2022) Volume, Effusion Rate, and Lava Transport During the 2021 Fagradalsfjall Eruption: Results From Near Real-Time Photogrammetric Monitoring. *Geophysical Research Letters* 49, e2021GL097125. https://doi.org/10.1029/2021GL097125

Pedersen, G.B.M., Belart, J.M.C., Óskarsson, B.V., Gunnarson, S.R., Gudmundsson, M.T., Reynolds, H.I., Valsson, G., Högnadóttir, T., Pinel, V., Parks, M.M., Drouin, V., Askew, R.A., Dürig, T., Þrastarson, R.H. (2024) Volume, effusion rates and lava hazards of the 2021, 2022 and 2023 Reykjanes fires: Lessons learned from near real-time photogrammetric monitoring. *EGU General Assembly 2024*, Vienna, Austria, 14–19 April 2024, Abstract EGU24-10724. https://doi.org/10.5194/egusphere-egu24-10724

Pfeffer, M.A., Bergsson, B., Barsotti, S., Stefánsdóttir, G., Galle, B., Arellano, S., Conde, V., Donovan, A., Ilyinskaya, E., Burton, M., Aiuppa, A., Whitty, R.C.W., Simmons, I.C., Arason, Þ., Jónasdóttir, E.B., Keller, N.S., Yeo, R.F., Arngrímsson, H., Jóhannsson, M.K., Askew, R.A., Dumont, S., Von Löwis, S., Ingvarsson, Þ., La Spina, A., Thomas, H., Prata, F., Grassa, F., Giudice, G., Stefánsson, A., Marzano, F., Montopoli, M., Mereu, L. (2018) Ground-Based Measurements of the 2014–2015 Holuhraun Volcanic Cloud (Iceland). *Geosciences* 8, 29. https://doi.org/10.3390/geosciences8010029

Ranta, E., Gunnarsson-Robin, J., Halldórsson, S.A., Ono, S., Izon, G., Jackson, M.G., Reekie, C.D.J., Jenner, F.E., Guðfinnsson, G.H., Jónsson, Ó.P., Stefánsson, A. (2022) Ancient and recycled sulfur sampled by the Iceland mantle plume. *Earth and Planetary Science Letters* 584, 117452. https://doi.org/10.1016/j.epsl.2022.117452

Ranta, E., Halldórsson, S.A., Óladóttir, B.A., Pfeffer, M.A., Caracciolo, A., Bali, E., Guðfinnsson, G.H., Kahl, M., Barsotti, S. (2024) Magmatic Controls on Volcanic Sulfur Emissions at the Iceland Hotspot. *EarthArXiv* Preprint v1. https://doi.org/10.31223/X51102

Sæmundsson, K., Sigurgeirsson, M.Á., Friðleifsson, G.Ó. (2020) Geology and structure of the Reykjanes volcanic system, Iceland. *Journal of Volcanology and Geothermal Research* 391, 106501. https://doi.org/10.1016/j.jvolgeores.2018.11.022

Schmidt, A., Leadbetter, S., Theys, N., Carboni, E., Witham, C.S., Stevenson, J.A., Birch, C.E., Thordarson, T., Turnock, S., Barsotti, S., Delaney, L., Feng, W., Grainger, R.G., Hort, M.C., Höskuldsson, Á., Ialongo, I., Ilyinskaya, E., Jóhannsson, T., Kenny, P., Mather, T.A., Richards, N.A.D., Shepherd, J. (2015) Satellite detection, long-range transport, and air quality impacts of volcanic sulfur dioxide from the 2014–2015 flood lava eruption at Bárðarbunga (Iceland). *Journal of Geophysical Research: Atmospheres* 120, 9739–9757. https://doi.org/10.1002/2015JD023638

Sigmundsson, F., Parks, M., Geirsson, H., Hooper, A., Drouin, V., Vogfjörd, K.S., Ófeigsson, B.G., Greiner, S.H.M., Yang, Y., Lanzi, C., De Pascale, G.P., Jónsdóttir, K., Hreinsdóttir, S., Tolpekin, V., Friðriksdóttir, H.M., Einarsson, P., Barsotti, S. (2024) Fracturing and tectonic stress drives ultra-rapid magma flow into dikes. *Science* 383, 1228–1235. https://doi.org/10.1126/science.adn2838

Sigurgeirsson, M.Á. (2004) Þáttur úr gossögu Reykjaness. *Náttúrufræðingurinn* 72, 21–28. https://timarit.is/gegnir/991000816469706886

Smythe, D.J., Wood, B.J., Kiseeva, E.S. (2017) The S content of silicate melts at sulfide saturation: New experiments and a model incorporating the effects of sulfide composition. *American Mineralogist* 102, 795–803. https://doi.org/10.2138/am-2017-5800CCBY

Stewart, C., Damby, D.E., Horwell, C.J., Elias, T., Ilyinskaya, E., Tomašek, I., Longo, B.M., Schmidt, A., Carlsen, H.K., Mason, E., Baxter, P.J., Cronin, S., Witham, C. (2022) Volcanic air pollution and human health:

recent advances and future directions. *Bulletin of Volcanology* 84, 11. https://doi.org/10.1007/s00445-021-01513-9

WEISER, F., BAUMANN, E., JENTSCH, A., MEDINA, F.M., LU, M., NOGALES, M., BEIERKUHNLEIN, C. (2022) Impact of Volcanic Sulfur Emissions on the Pine Forest of La Palma, Spain. *Forests* 13, 299. https://doi.org/10.3390/f13020299

WIESER, P.E., GLEESON, M. (2022) PySulfSat: An open-source Python3 tool for modeling sulfide and sulfate saturation. *Volcanica* 6, 107–127. https://doi.org/10.30909/vol.06.01.107127

Medieval and recent SO₂ budgets in the Reykjanes Peninsula: implication for future hazard

A. Caracciolo, E. Bali, E. Ranta, S.A. Halldórsson, G.H. Guðfinnsson, B.V. Óskarsson

Supplementary Information

The Supplementary Information includes:

Calculation of SO₂ Emissions

The total mass of sulfur (M_S, [kg]) which was released from the magma and dispersed into the atmosphere can be calculated as:

$$M_S = V_{DRE} \times \rho \times \Delta C_S \,, \qquad (S\text{-}1)$$

where V_{DRE} is the dense rock equivalent volume (vesicle-free) of the erupted lava unit in m³, ρ is the density of the melt in kg/m³ and ΔC_S the mass of sulfur release *per* unit mass of melt. Particularly, ΔC_S is calculated as:

$$\Delta C_S = (1 - X)\,(C_{S\,MI} - C_{S\,glass}) \,, \qquad (S\text{-}2)$$

where X is the crystal content of the lava, which is set at 0.02. This is a reasonable and conservative assumption as the 800–1240 AD Fires contain little amount of macrocrysts, <2 vol. % (Caracciolo *et al*., 2023). $C_{S\,MI}$ and $C_{S\,glass}$ are the pre-eruptive and post-erupted sulfur (S) concentrations for a given eruption, respectively, which in this work were chosen as the maximum and minimum S concentrations measured in MIs and in tephra glasses, respectively (*cf*. Table 1). The volume of the erupted lava unit is expressed as dense rock equivalent (V_{DRE}), which reflects the volume of the vesicle-free lava. However, published lava volumes for the 800–1240

AD Fires refer to bulk volumes and do not take into account the porosity of the lava. For this reason, we estimated V_{DRE} by multiplying the bulk volume (V) for a scaling factor that accounts for vesicularity (0.85 in this work). Due to the lack of vesicularty data for the lava units targeted in this study and considering that vesicularity is highly variable across basaltic lava flows (*e.g.*, Cashman and Kauahikaua, 1997), we use a bulk vesicularity of 15 %, consistent with findings for the 2014–2015 Holuhraun lava flow (Bonny *et al.*, 2018). This bulk vesicularity is within the range of vesicularity constrained for other basaltic lava flows in Iceland, such as Hafnarhraun in the Reykjanes peninsula (12–37 % vesicularity; Nikkola *et al.*, 2019) and Vikrahraun, the 1961 lava flow from Askja (0–30 % vesicularity; Blasizzo *et al.*, 2022).

Assessing the daily SO_2 emissions of past eruptions is challenging, particularly for those eruptions where the duration is unknown, such as for the 800–1240 AD Fires. We calculated daily SO_2 emissions [kg/d] starting from MOR values using the following equation:

$$\text{Daily } SO_2 \text{ emissions} = MOR_i \times \rho \times (\Delta C_S \times 2) \times 86{,}400 \ . \text{ (S-3)}$$

Additionally, in Table 1 we included the amount of time required to erupt and emplace a specific volume of magma, which can be used as a proxy for eruption durations. We call this time of lava emplacement. In fact, we cannot rule out that erupted volumes reflect multiple eruptive phases over which the lava was emplaced, as observed during the 2023–2024 Svartsengi eruptions (<48 h) and as suggested by Caracciolo *et al.* (2023). The time of lava emplacement (t_m [days]) of each eruptive unit was calculated by using MOR values calculated by Óskarsson *et al.* (2024) (Table 1), using the following equation:

$$t_m = \frac{V_i}{MOR_i \times 86{,}400}, \qquad\qquad \text{(S-4)}$$

where V_i [m³] and MOR_i [m³/s] are the bulk volume and the MOR of a specific lava unit, respectively. The time of lava emplacement for the new 2021–2024 eruptions at Fagradalsfjall and Svartsengi represents the actual duration of each eruption. Óskarsson *et al.* (2024) calculate mean output rates (MOR) and uncertainty ranges for each eruption targeted in this work. Therefore, the time of lava emplacement and daily SO_2 emissions for each eruption was calculated taking into account the uncertainty range in MOR values (Table 1).

Modelling Sulfur Degassing

Sulfur degassing was modelled using the open source COHS-degassing model Sulfur_X (Ding *et al.*, 2023), using the COH model of Newman and Lowenstern (2002) and the S speciation model of O'Neill and Mavrogenes (2022). Oxygen fugacity was set at $\Delta FMQ = 0$ (Novella *et al.*, 2020) and $T = 1200$ °C. Pre-eruptive S concentration was chosen as 1550 ppm based on MI data, whereas H_2O and CO_2 concentrations were estimated at 0.3 wt. % and 1000 ppm, respectively, in agreement with typical H_2O and CO_2 concentrations of Icelandic rift basalts (*e.g.*, Bali *et al.*, 2018; Halldórsson *et al.*, 2022). Melt composition was chosen as the mean groundmass glass compositions of the 800–1240 AD Fires. We also tested S degassing of hypothetical scenarios with higher melt H_2O contents of 1.5 wt. % and 3 wt. %, unrealistically high for Iceland rift basalts (Ranta *et al.*, 2024). Higher H_2O contents push the onset of S degassing to higher pressures.

However, >3 wt. % H_2O contents are required for significant S degassing to occur at known magma storage depths.
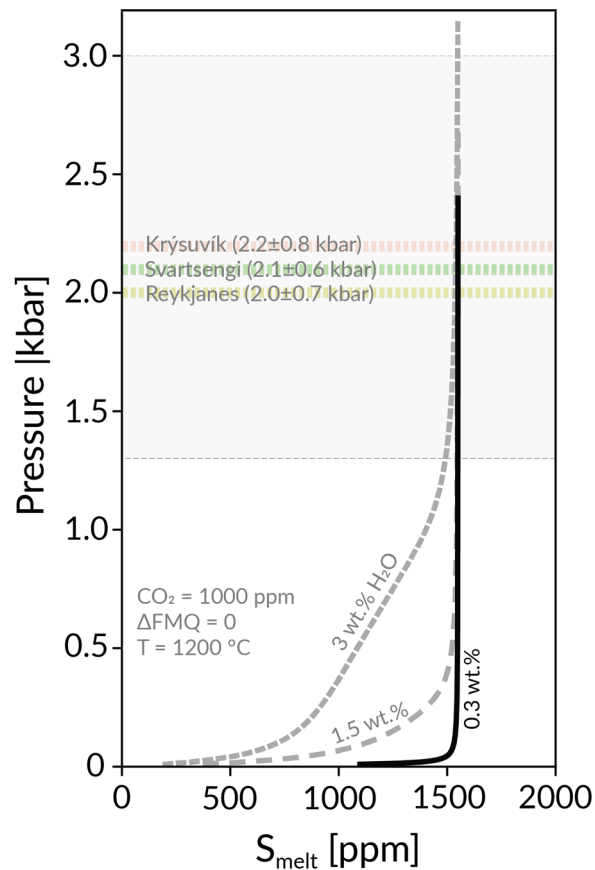

Figure S-1   Models of melt S degassing as a function of pressure. Thick black curve indicates realistic H_2O contents for Reykjanes basalts. Dashed grey lines indicate S degassing assuming unrealistically high H_2O contents of 1.5 and 3 wt. %. Modelling was carried out using Sulfur_X (Ding *et al.*, 2023).

The Occurrence of Degassed and Partially Degassed Melt Inclusions

Many melt inclusion compositions from Brennisteinsfjöll, and to a lesser extent, from Svartsengi, are found to be partially to fully degassed (Fig. 1). In the case of Brennisteinsfjöll, in which we have a larger amount of partially and fully degassed MIs, individual crystals contain multiple MIs with variable S contents. Within the same crystal, some MIs have 'normal' S contents (>1200 ppm) consistent with fractional crystallisation trends, whereas some are partially (400–1100 ppm S) degassed (Fig. 1). Additionally, some MIs are completely degassed, with S contents similar to groundmass values (<400 ppm) (Fig. 1d). Based on backscattered electron (BSE) images, those MIs that are partially to completely degassed contain very large bubbles (Fig. S-2). Post-entrapment degassing at low-*P* (*e.g.*, during eruption) could be responsible for the observed partially to completely degassed MIs in Brennisteinsfjöll. The MIs could release S at low pressure, such as when a host

crystal fractures during an eruption, causing the pressure within certain MIs to rapidly decrease to nearly atmospheric. In this scenario, the melt within the MIs degasses sulfur into the shrinkage bubble prior to quenching.
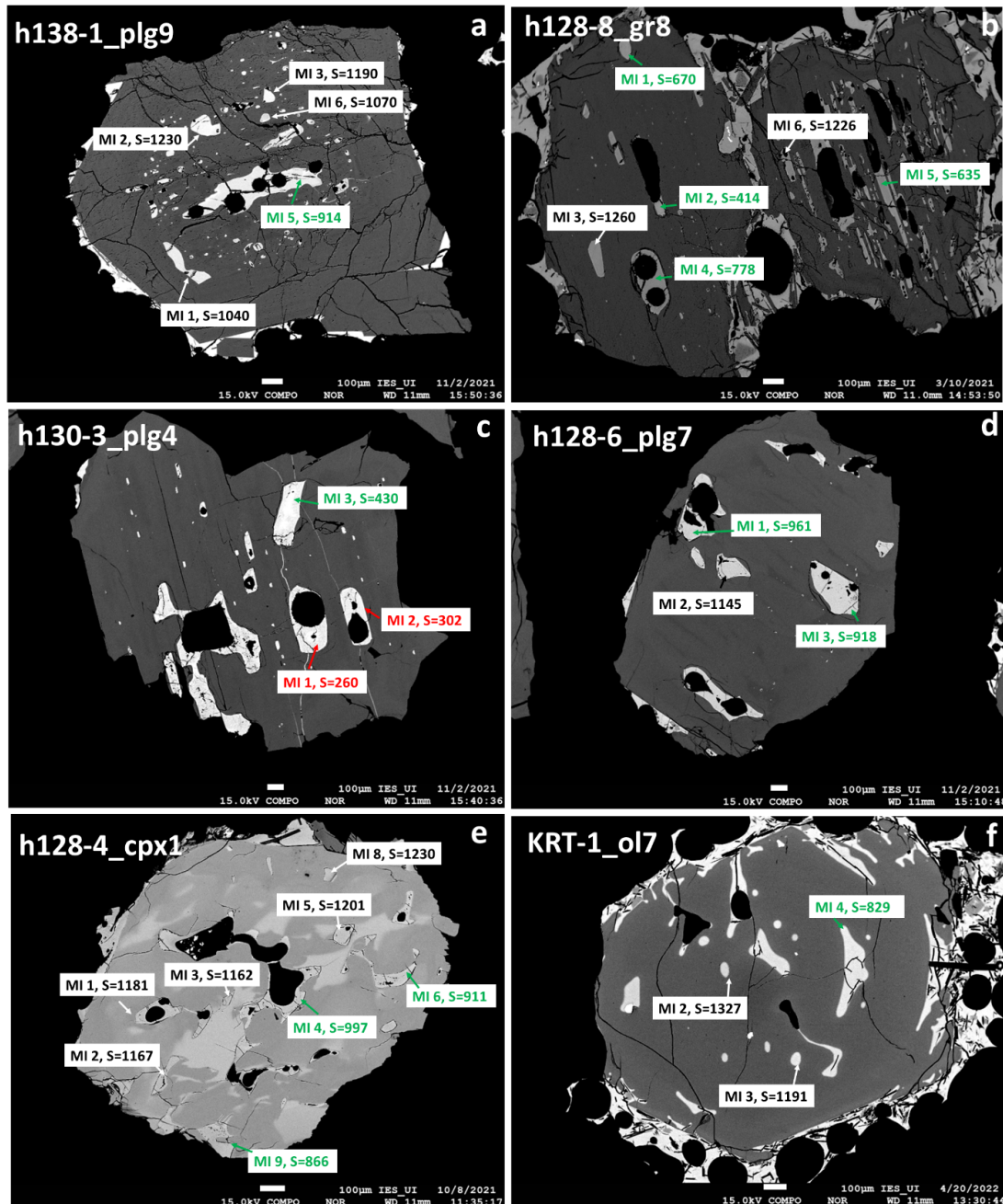

Figure S-2 BSE images of **(a–d)** plagioclase, **(e)** clinopyroxene and **(f)** olivine crystals from Brennisteinsfjöll containing multiple MIs with different S contents. Note that partially and completely degassed MIs contain large bubbles, which probably contained S-bearing mineral precipitates which sequestered a significant amount of S.

Selection of Enriched and Depleted End Member Melt Compositions

End member melt compositions were selected from the MI record preserved in the 800–1240 AD Fires and using K_2O/TiO_2 as a proxy for magma enrichment, which has been proven to be a robust tracer of mantle-derived chemical variability (Halldórsson *et al.*, 2022; Harðardóttir *et al.*, 2022). For the depleted end member melt composition, the MI dataset was filtered by selecting and averaging PEP-corrected MI compositions (*n* = 3) satisfying the following criteria: $K_2O/TiO_2 < 0.1$, Mg# > 70 and MgO > 9 wt. %. The resulting melt composition has Mg# = 70.4, 9.5 wt. % MgO and S content of 680 ± 85 ppm. The enriched end member melt composition was chosen by averaging MI compositions (*n* = 4) satisfying the following criteria: Mg# > 69, MgO > 9 wt. %, $K_2O/TiO_2 > 0.3$ and $TiO_2 > 0.4$ wt. %. The resulting composition has Mg# = 70, 9.8 wt. % MgO and S content of 872 ± 166 ppm. Starting from these initial compositions, we modelled fractional crystallisation using Petrolog3 (Danyushevsky and Plechov, 2011) at 2 kbar and at fO$_2$ corresponding to the FMQ buffer. S partition coefficient between melt and olivine, plagioclase and clinopyroxene were taken from Callegaro *et al.* (2020) (S partition coefficient of Cpx–melt = 0.05, Olivine–melt = 0.01, Plagioclase–melt = 0.13).

Modelling SCSS

Sulfur concentration at sulfide saturation (SCSS) was modelled along an empirical fractional crystallisation path calculated between Mg# = 75 and Mg# = 40 by regressing the observed MI and glass data with linear functions for each volcanic system. Melt temperature was calculated using the melt-only thermometer (Eq. 14 in Putirka, 2008). SCSS modelling was implemented in PySulfSat (Wieser and Gleeson, 2022), by comparing different SCSS models (Fortin *et al.*, 2015; Smythe *et al.*, 2017; O'Neill and Mavrogenes, 2022) (Fig. S-2). For the modelling parameters, we used $Fe^{3+}/Fe^{tot} = 0.1$, P = 2 kbar and sulfide Fe/(Fe+Ni+Cu) = 0.65. The different models yield similar results and well within the 1σ uncertainty of the Smythe *et al.* (2017) model (see Fig. S-3a–d).
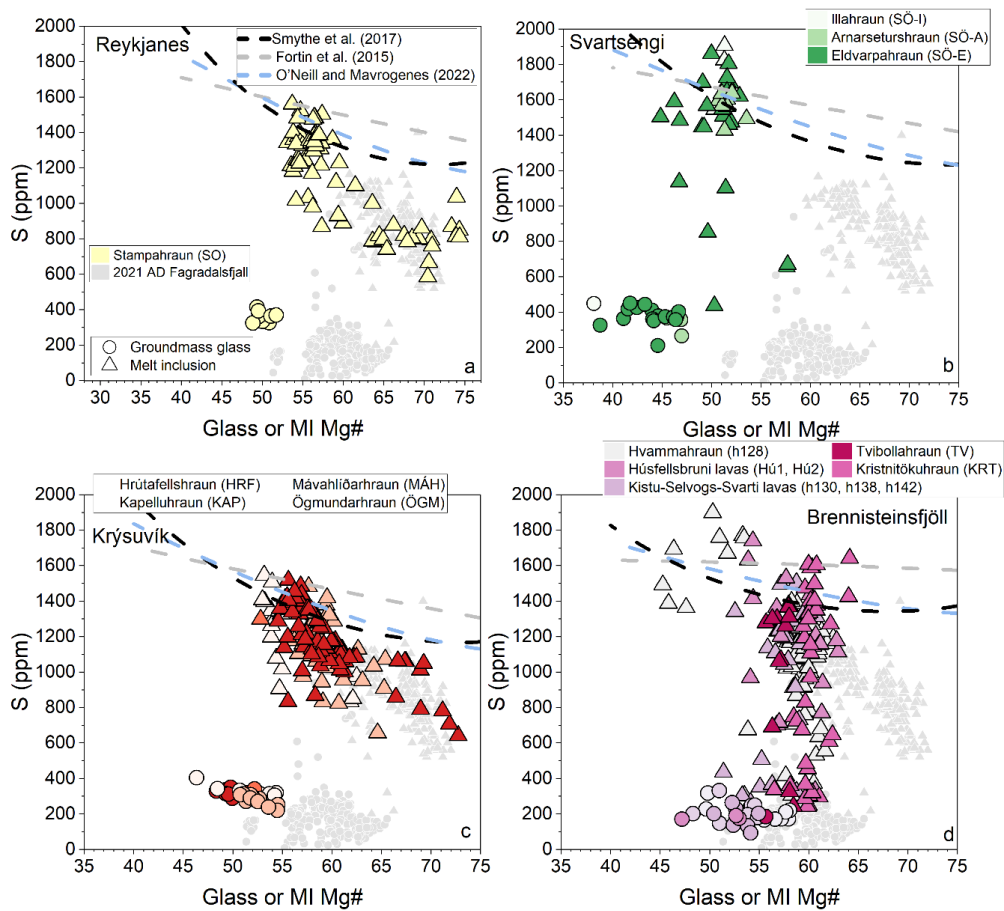
Figure S-3 Variation of S contents in groundmass glasses (filled circles) and PEP-corrected MIs (filled triangles) as a function of Mg# in samples from the 800–1240 AD Fires and the 2021 Fagradalsfjall eruption. The purpose of the figure is to compare results from different SCSS models, indicated with different dashed curves.

Figure S-4 [next page] **(a–d)** Variation of S contents in groundmass glasses (filled circles) and PEP-corrected MIs (filled triangles) as a function of Mg# [Mg# = $100 \cdot Mg/(Mg+Fe^{2+})$, $Fe^{2+}/Fe^{tot} = 0.9$] in samples from the 800–1240 AD Fires and raw MI data from the December 2023, January 2024 and February 2024 Sundhnúkuar eruptions. Data from the 2021 AD Fagradalsfjall eruption are from Halldórsson *et al.* (2022). Red and blue solid lines indicate fractional crystallisation paths calculated for a geochemically enriched and depleted initial melt compositions, respectively. The black dashed curve indicates SCSS along an empirical fractional crystallisation path calculated after Smythe *et al.* (2017). **(e–h)** Measured MI S contents *vs.* calculated SCSS, coloured after MgO content. SCSS was calculated assuming $Fe^{3+}/Fe^{tot} = 0.1$, $P = 2$ kbar, $T = 1220\,°C$ and sulfide $Fe/(Fe+Ni+Cu) = 0.65$, after the method of Smythe *et al.* (2017) (*cf.* Fig. S-3). All SCSS models were implemented in PySulfSat code (Wieser and Gleeson, 2022).
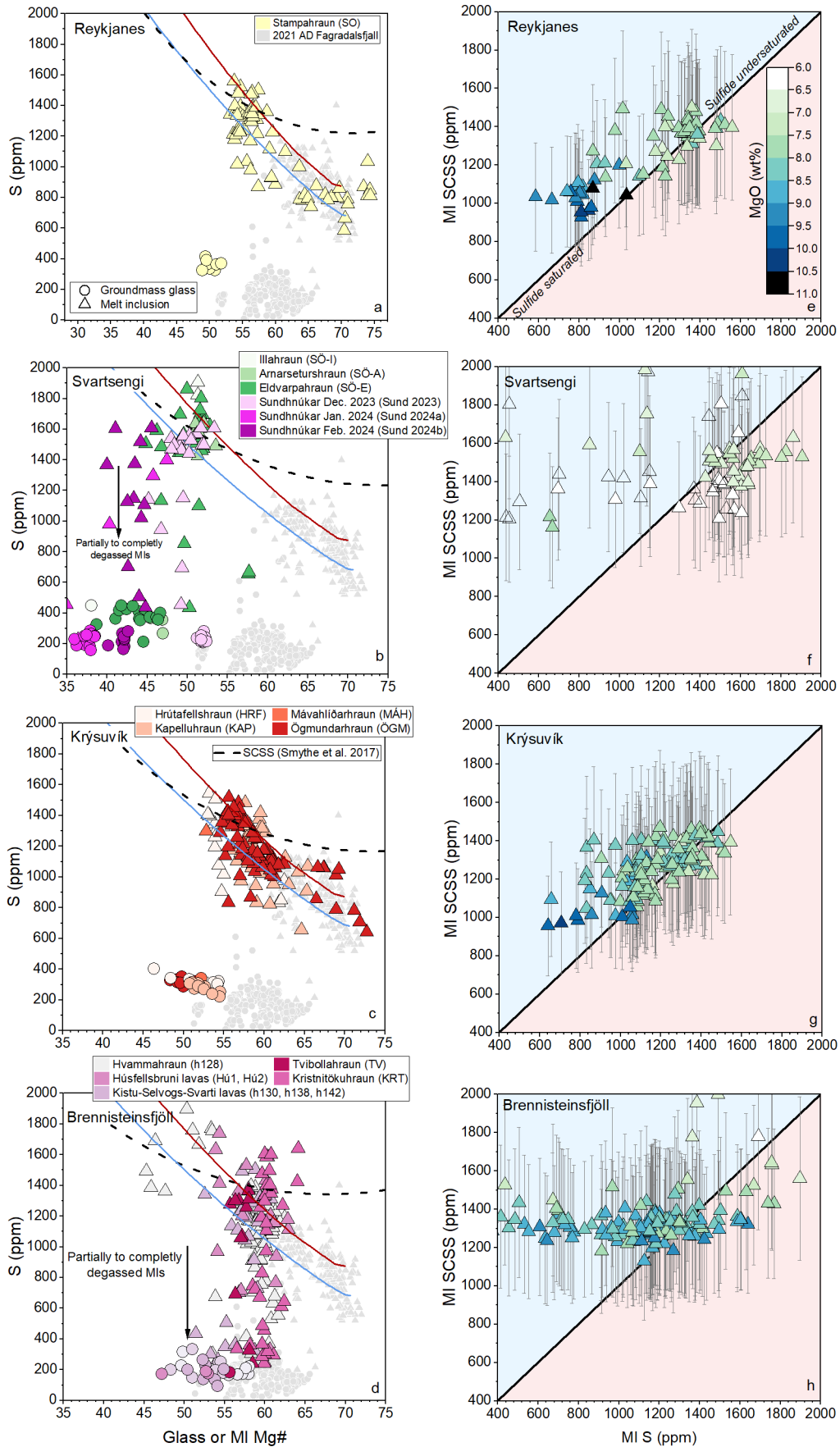
Supplementary Tables

The MI and glass dataset published in this work complement the dataset published in Caracciolo *et al*. (2023) and here includes S and Cl measurements. Re-homogenized melt inclusions are not included in this work. Additionally, the dataset includes new groundmass and MI data from the data from the 2022–2023 Fagradalsfjall eruptions and the 2023–2024 eruptions at Sundhnúksgígar in Svartsengi.

Table S-1   Overview of samples studied in this work, along with acronyms, lava flows, ages and coordinates. Analysed phases in each sample are indicated with cross marks.

Table S-2   Groundmass glass dataset.

Table S-3   Mean compositions of groundmass glasses and glass standards.

Table S-4   Melt inclusion dataset listing PEP-corrected and raw compositions, along with host mineral compositions and 1σ uncertanties. Note that MIs from the 2023 Fagradalsfjall eruption and the December 2023 and January 2024 Sundhnúksgígar eruptions have not been PEP-corrected.

Tables S-1 to S-4 are available for download (.xlsx) from the online version of this article at http://doi.org/10.7185/geochemlet.2417.

Supplementary Information References

Bali, E., Hartley, M.E., Halldórsson, S.A., Gudfinnsson, G.H., Jakobsson, S. (2018) Melt inclusion constraints on volatile systematics and degassing history of the 2014–2015 Holuhraun eruption, Iceland. *Contributions to Mineralogy and Petrology* 173, 9. https://doi.org/10.1007/s00410-017-1434-1

Blasizzo, A.Y., Ukstins, I.A., Scheidt, S.P., Graettinger, A.H., Peate, D.W., Carley, T.L., Moritz, A.J., Thines, J.E. (2022) Vikrahraun—the 1961 basaltic lava flow eruption at Askja, Iceland: morphology, geochemistry, and planetary analogs. *Earth, Planets and Space* 74, 168. https://doi.org/10.1186/s40623-022-01711-5

Bonny, E., Thordarson, T., Wright, R., Höskuldsson, A., Jónsdóttir, I. (2018) The Volume of Lava Erupted During the 2014 to 2015 Eruption at Holuhraun, Iceland: A Comparison Between Satellite- and Ground-Based Measurements. *Journal of Geophysical Research: Solid Earth* 123, 5412–5426. https://doi.org/10.1029/2017JB015008

Callegaro, S., Geraki, K., Marzoli, A., de Min, A., Maneta, V., Baker, D.R. (2020) The quintet completed: The partitioning of sulfur between nominally volatile-free minerals and silicate melts. *American Mineralogist* 105, 697–707. https://doi.org/10.2138/am-2020-7188

Caracciolo, A., Bali, E., Halldórsson, S.A., Guðfinnsson, G.H., Kahl, M., Þórðardóttir, I., Pálmadóttir, G.L., Silvestri, V. (2023) Magma plumbing architectures and timescales of magmatic processes during

historical magmatism on the Reykjanes Peninsula, Iceland. *Earth and Planetary Science Letters* 621, 118378. https://doi.org/10.1016/j.epsl.2023.118378

Cashman, K.V., Kauahikaua, J.P. (1997) Reevaluation of vesicle distributions in basaltic lava flows. *Geology* 25, 419–422. https://doi.org/10.1130/0091-7613(1997)025<0419:ROVDIB>2.3.CO;2

Danyushevsky, L.V., Plechov, P. (2011) Petrolog3: Integrated software for modeling crystallization processes. *Geochemistry, Geophysics, Geosystems* 12, Q07021. https://doi.org/10.1029/2011GC003516

Ding, S., Plank, T., Wallace, P.J., Rasmussen, D.J. (2023) Sulfur_X: A Model of Sulfur Degassing During Magma Ascent. *Geochemistry, Geophysics, Geosystems* 24, e2022GC010552. https://doi.org/10.1029/2022GC010552

Fortin, M.-A., Riddle, J., Desjardins-Langlais, Y., Baker, D.R. (2015) The effect of water on the sulfur concentration at sulfide saturation (SCSS) in natural melts. *Geochimica et Cosmochimica Acta* 160, 100–116. https://doi.org/10.1016/j.gca.2015.03.022

Halldórsson, S.A., Marshall, E.W., Caracciolo, A., Matthews, S., Bali, E., Rasmussen, M.B., Ranta, E., Robin, J.G., Guðfinnsson, G.H., Sigmarsson, O., Maclennan, J., Jackson, M.G., Whitehouse, M.J., Jeon, H., van der Meer, Q.H.A., Mibei, G.K., Kalliokoski, M.H., Repczynska, M.M., Rúnarsdóttir, R.H., Sigurðsson, G., Pfeffer, M.A., Scott, S.W., Kjartansdóttir, R., Kleine, B.I., Oppenheimer, C., Aiuppa, A., Ilyinskaya, E., Bitetto, M., Giudice, G., Stefánsson, A. (2022) Rapid shifting of a deep magmatic source at Fagradalsfjall volcano, Iceland. *Nature* 609, 529–534. https://doi.org/10.1038/s41586-022-04981-x

Harðardóttir, S., Matthews, S., Halldórsson, S.A., Jackson, M.G. (2022) Spatial distribution and geochemical characterization of Icelandic mantle end-members: Implications for plume geometry and melting processes. *Chemical Geology* 604, 120930. https://doi.org/10.1016/j.chemgeo.2022.120930

Newman, S., Lowenstern, J.B. (2002) VolatileCalc: a silicate melt–H_2O–CO_2 solution model written in Visual Basic for excel. *Computers & Geosciences* 28, 597–604. https://doi.org/doi:10.1016/S0098-3004(01)00081-4

Nikkola, P., Thordarson, T., Rämö, O.T., Heikkilä, P. (2019) Formation of segregation structures in Hafnarhraun pāhoehoe lobe, SW Iceland: a window into crystal–melt separation in basaltic magma. *Bulletin of Volcanology* 81, 70. https://doi.org/10.1007/s00445-019-1330-9

Novella, D., Maclennan, J., Shorttle, O., Prytulak, J., Murton, B.J. (2020) A multi-proxy investigation of mantle oxygen fugacity along the Reykjanes Ridge. *Earth and Planetary Science Letters* 531, 115973. https://doi.org/10.1016/j.epsl.2019.115973

O'Neill, H.St.C., Mavrogenes, J.A. (2022) The sulfate capacities of silicate melts. *Geochimica et Cosmochimica Acta* 334, 368–382. https://doi.org/10.1016/j.gca.2022.06.020

Óskarsson, B.V. , Askew, R.A., Guðmundsson, H. (2024) Assessing the mean output rate (MOR) of past effusive basaltic eruptions - a look at the postglacial volcanism of the Reykjanes Peninsula in Iceland. *EarthArXiv* Preprint v1. https://doi.org/10.31223/X5CH68

Putirka, K.D. (2008) Thermometers and Barometers for Volcanic Systems. *Reviews in Mineralogy and Geochemistry* 69, 61–120. https://doi.org/10.2138/rmg.2008.69.3

Ranta, E., Halldórsson, S.A., Óladóttir, B.A., Pfeffer, M.A., Caracciolo, A., Bali, E., Guðfinnsson, G.H., Kahl, M., Barsotti, S. (2024) Magmatic Controls on Volcanic Sulfur Emissions at the Iceland Hotspot. *EarthArXiv* Preprint v1. https://doi.org/10.31223/X51102

Smythe, D.J., Wood, B.J., Kiseeva, E.S. (2017) The S content of silicate melts at sulfide saturation: New experiments and a model incorporating the effects of sulfide composition. *American Mineralogist* 102, 795–803. https://doi.org/10.2138/am-2017-5800CCBY

Wieser, P.E., Gleeson, M. (2022) PySulfSat: An open-source Python3 tool for modeling sulfide and sulfate saturation. *Volcanica* 6, 107–127. https://doi.org/10.30909/vol.06.01.107127